Automatic Detection of Stimulation Artifacts to Isolate Volitional from Evoked EMG Activity

Available online at www.sciencedirect.com

ScienceDirect

IFAC PapersOnline CONFERENCE PAPER ARCHIVE

IFAC PapersOnLine 51-27 (2018) 282–287

Automatic Detection of Stimulation Artifacts to Isolate Volitional from Evoked EMG Activity ⋆

Ana Carolina C. de Sousa [*,**] **Markus Valtin** [*]
Antônio P. L. Bó [**] **Thomas Schauer** [*]

[*] *Control Systems Group, Technische Universität Berlin, Berlin, Germany (e-mail: {schauer,valtin}@control.tu-berlin.de)*
[**] *Department of Electrical Engineering, University of Brasilia, Campus Darcy Ribeiro, Brazil (e-mail: {anacsousa,antonio.plb}@lara.unb.br).*

Abstract: Control systems for human physiotherapy exercises based on functional electrical stimulation (FES) have provided excellent performance in several setups. Myocontrolled neuroprostheses use electromyography (EMG) for timing and intensity control of stimulation applied to these exercises, estimating not only the volitional activity (from the patient) but also the evoked activity (from FES). A typical EMG response to FES starts with the stimulation artifact, followed by an excitation curve called M-wave. To extract volitional and evoked components, we first need to find the inter-pulse-intervals (IPIs), i.e., the EMG signal between stimulation artifacts. For that, we have developed a method for two-channel stimulation artifact detection for EMG signals which are not hardware-synchronized to a FES stimulator. First, the artifact detection approach marks all potential artifacts based on one of three adaptive threshold-based detection methods (mean/standard deviation, median/MAD and quantiles). Subsequently, for IPI extraction we cluster the potential stimulation artifacts to cross-correlate the resulting potential stimulation artifact vector with a vector of expected artifacts based on the stimulation and EMG frequencies. For evaluation, we performed tests on two benchmark datasets obtained from FES-assisted walking with two hardware setups. We found more than 95% success rate for both hardware setups using the adaptive threshold method independently on the selected method for choosing the threshold. Because of its low computational demands, we recommend the mean/standard deviation approach.

Keywords: Electrical stimulation, Neural control, Electromyography, Artifact detection, Myocontrolled neuroprosthetics.

1. INTRODUCTION

Technology advances improved physiotherapy techniques for movement restoration of individuals with lower limb disability, such as stroke and spinal cord injury (SCI). Functional electrical stimulation (FES) stands for a known rehabilitation technique for motor functions improvement, in which FES generates muscle contraction (Lynch and Popovic, 2012). For timing and intensity control of stimulation, FES systems usually measure position, velocity, and torque. Although these variables are sometimes straightforward to measure and to process, it is harder to differentiate evoked (i.e., from FES) from volitional activity (i.e., from the patient). Therefore, electromyography (EMG) measurements for feedback control of timing and intensity of stimulation may provide more efficient rehabilitation protocols (Schauer, 2017).

After a stimulation pulse, a typical EMG response starts with the stimulation artifact, a spike lasting between less than a millisecond and a couple of milliseconds, followed by an excitation curve, called M-wave. The latter is formed by the synchronous muscle action potentials (MAP) of all motor units that have been fired by the stimulation pulse. The Gaussian-like superposition of MAPs caused by volitional muscle activation is much smaller than the artifact and M-wave. To extract these components from EMG signals, we need first to find the inter-pulse-intervals (IPIs), i.e., the EMG signal between stimulation artifacts.

Many previous projects precisely synchronized the EMG amplifier and the stimulator during stimulation to reduce (e.g., (Thorsen, 1999)) or even completely remove (e.g., (Knaflitz and Merletti, 1988; Shalaby et al., 2011)) artifacts by custom-made hardware interfaces. The synchronization allows the precise suppression, blanking or marking of stimulation pulses in the EMG recordings.

⋆ We would like to thank the Coordenação de Aperfeiçoamento de Pessoal de Nível Superior (Capes/MEC) for providing financial support for this work. In addition, this work was partially funded by the European project RETRAINER (Horizon 2020, Research and Innovation Programme, grant agreement No 644721). The used stimulation electrodes were donated by Axelgaard Manufacturing Co., USA.

10.1016/j.ifacol.2018.11.628

Other researchers used separate stimulation and EMG measurement devices. A loose synchronization between EMG recording and stimulation was achieved by controlling the pulse generation and EMG recording within one software on the PC. This setup hinders a precise marking of stimulation artifacts – only the presence of an artifact can be assumed within a given time window. Additional signal processing steps are required to precisely detect the onset of the stimulation artifacts and to extract the last complete inter-pulse-interval (IPI) or the EMG data after the last detected stimulation artifact (incomplete IPI). (Soares et al., 2013; Klauer et al., 2012) calculated the cross-correlation function between the EMG signal and an artifact template to locate potential artifact onsets. However, finding a suitable artifact template is a challenge when stimulating more than one channel on a limb. Most stimulation devices possess only one current source and generate the pulses on the different channels time-multiplexed in a fast sequence. Threshold-based artifact detection serves as another possible approach to find stimulation artifacts. The threshold is often chosen based on statistical signal properties like standard deviation and median absolute deviation (MAD). However, manual adaptation is usually required. More sophisticated methods use Wavelet transformations to calculate thresholds (Merlo et al., 2003; Arafat and Skubic, 2008), yet, these calculations require much computation time and fine tuning of a large number of parameters. Finally, machine learning might be applied to detect stimulation artifacts.

This paper describes and evaluates different methods for detecting stimulation artifacts for two channels of EMG and stimulation on the same limb segment. Such a setup is of practical relevance, e.g., when controlling a body joint by one pair of antagonistic muscles. We aimed to develop and provide a SIMULINK® (The Mathworks Inc., USA) toolbox for EMG processing during FES that can be used with different non-hardware-synchronized stimulators and EMG amplifies for various EMG sampling frequencies and stimulation rates. The artifact detection approach considered in this paper contains two phases: first, an adaptive threshold-based detection will mark all potential artifacts, and then a clustering/cross-correlation approach combined with a plausibly check will extract the last complete or incomplete IPI. Afterward, we feed the extracted IPIs to filters for estimating volitional and evoked EMG activity. The toolbox was tested on benchmark data obtained from FES-assisted walking with two different EMG systems in which the number of active channels, as well as the form and intensity of the stimulation artifacts, varies over time.

Section 2 presents an overview on the proposed methods followed by the experimental evaluation in Section 3. The obtained results are presented in Section 4 before the final discussion and conclusions in Section 5.

2. METHODS

The stimulation artifact detection is executed at stimulation frequency and must consider that noise, poor cable connection and movements also generate EMG artifacts. In this paper, we present a method that starts buffering two vectors with M raw EMG samples (one buffer for each channel). The buffer size should be $M > L$ for searching

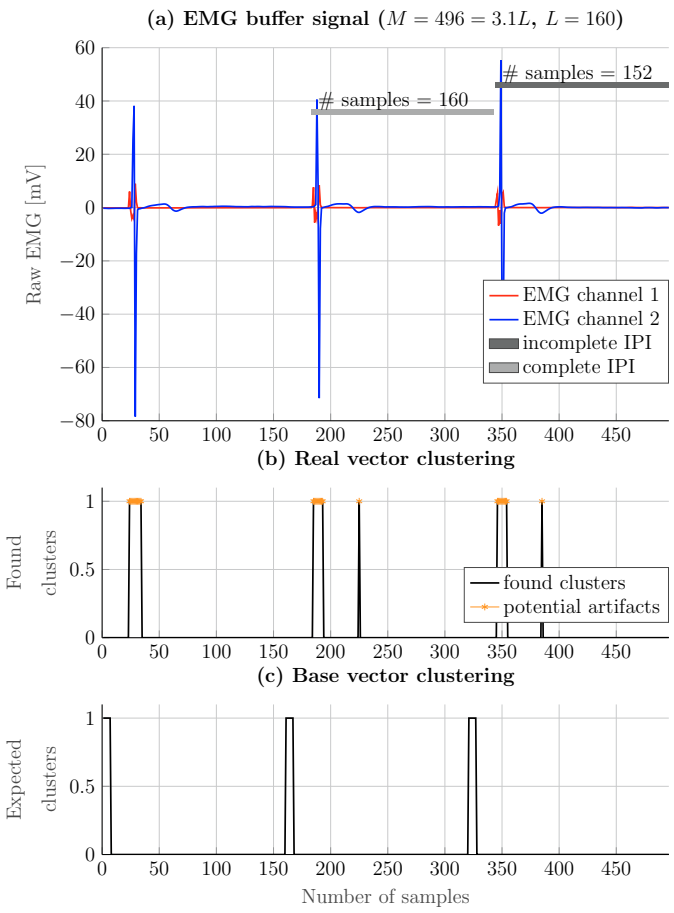

Fig. 1. Clustering potential artifacts. (a) EMG buffer with complete and incomplete EMG vectors marked. (b) Potential artifacts clustering yields the real vector v_r. (c) Base vector with expected stimulation artifacts.

the last incomplete IPI and $M > 2L$ for searching the last complete IPI. Here, L corresponds to the expected number of EMG samples between two stimulation pulses. L is defined by the frequency of EMG ($f_e = \{1\text{kHz}, 2\text{kHz}, 4\text{kHz}\}$) and stimulation ($f_s = \{25\text{Hz}, 40\text{Hz}, 50\text{Hz}\}$) as

$$L = \left\lceil \frac{f_e}{f_s} \right\rceil . \tag{1}$$

Even larger buffer sizes might be chosen if the computational power allows it. The influence of the buffer size on the detection rate will be discussed later. Note that M must be chosen in a way that we know the number of expected stimulation pulses inside the buffer (loose synchronization of FES and EMG). As illustrated in Fig. 1, for a buffer that contains $M = \lceil 3.1L \rceil$ samples we expect at least three stimulation artifacts during active FES. At each stimulation instant k, the EMG amplifier transmits EMG vectors with up to L samples to the artifact detection block for both EMG-channels. The built raw EMG buffer vectors are

$$\mathbf{b}_c[k] = [b_{c,1}[k] \ \dots \ b_{c,M}[k]]^T , \tag{2}$$

where $c \in \{1, 2\}$ stands for the EMG channel. $b_{c,M}[k]$ represents the most recent EMG samples available in the SIMULINK block for artifact detection.

During execution, the block considers that EMG and stimulator frequencies are constant and hardware dependent. Beforehand, the user declares both frequencies, considering also the application (cf. Sec. 2.3, e.g., performing both volitional and evoked estimation requires a lower stimulation frequency, e.g. $f_s = 25$ Hz, whereas only volitional EMG estimation is also possible for higher stimulation frequencies up to 50 Hz). The user also chooses which potential artifact detection algorithm will be applied, and which IPI vector should be returned, the last complete or the recent incomplete one (see Fig. 1(a)). The block returns the corresponding IPI when stimulation is active (stimulation intensity (charge) of any channel $q_i > 0, i \in 1, 2$) or the most recent L EMG samples when the stimulation is off ($q_i = 0$), $i =\in 1, 2$). The stimulation intensities are therefore additional inputs to the artifact detection block.

2.1 Detection of potential stimulation artifacts

When stimulation is active, the block marks all potential artifacts by one of the three algorithms available based on some EMG signal properties (mean/standard deviation, median/median absolute deviation (MAD) or quantiles). To remove offsets and to amplify the high-frequency signal components we compute the second-order differences in each EMG channel buffer. Thus, for $\mathbf{b_1}$ and $\mathbf{b_2}$ at each instant k, we obtain

$$\begin{aligned} \mathbf{B_1} &= \Delta^2 \mathbf{b}_1, \\ \mathbf{B_2} &= \Delta^2 \mathbf{b}_2. \end{aligned} \tag{3}$$

From $\mathbf{B_1}$ and $\mathbf{B_2}$, we compute two thresholds ($th_{\max,c}$ and $th_{\min,c}$) for each channel $c \in \{1, 2\}$, depending on the method explained below. Finally, we mark all EMG sampling instances i for of buffers that fulfill the criterion

$$B_{c,i} > th_{max,c} \text{ or } B_{c,i} < th_{min,c}, \tag{4}$$

and join the resulting sets of time points from both channels. $B_{c,i}, i = \{1, \ldots, M\}$ are the elements of the vector $\mathbf{B}_c$ for channel $c \in \{1, 2\}$. This method takes into account that most stimulators have one current source that generates pulses on two channels sequentially in a short period of time. In addition, the method also foresees that pulses of each stimulation channel will be visible in both EMG channels due to the close proximity of all electrodes at one limb segment.

Defining thresholds by mean and standard deviation The most intuitive method considers the means $\overline{B_1}$ and $\overline{B_2}$ and standard deviations σ_1 and σ_2 of the vectors $\mathbf{B_1}$ and $\mathbf{B_2}$, respectively. Then, the maximum and minimum thresholds are defined as

$$\begin{aligned} th_{max_c} &= \overline{B_c} + \alpha\sigma_c, \\ th_{min_c} &= \overline{B_c} - \alpha\sigma_c, \end{aligned} \tag{5}$$

where $\alpha > 0$ is a tuning parameter. Red lines in Fig. 2 illustrate an example of maximum and minimum thresholds using mean and variance for $\alpha = 3$.

Defining thresholds by median and MAD Since both the mean and the standard deviation are particularly sensitive to outliers, the median value m becomes a more suitable estimator than the mean (Leys et al. (2013)). The median absolute deviation (MAD) is also a considerable estimation

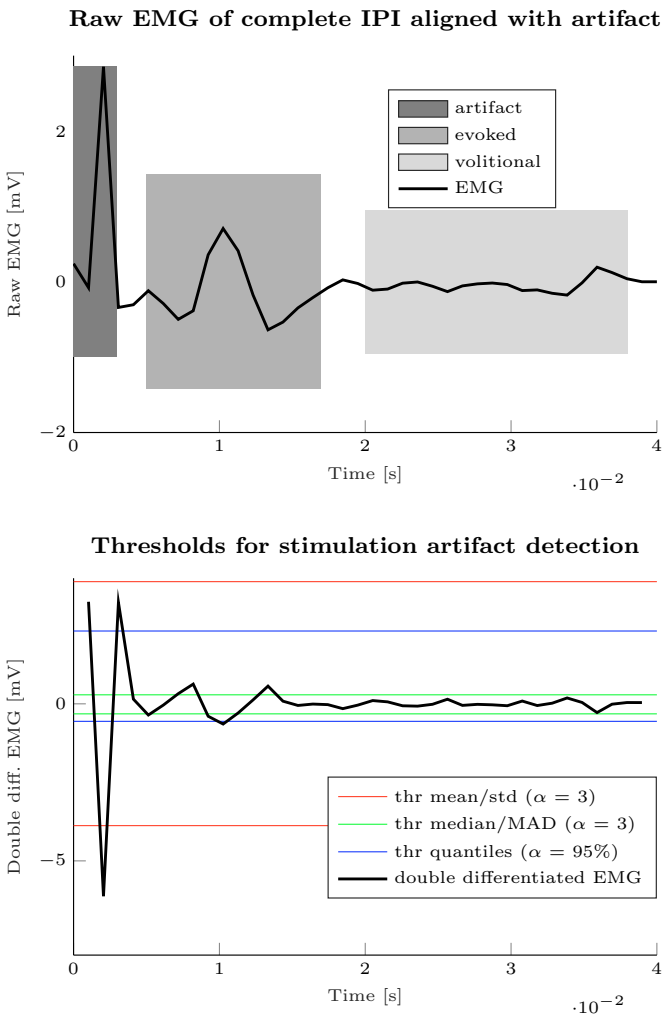

Fig. 2. Extracted IPI of EMG, dark gray marks the region of the artifact, medium gray marks the region of M-wave, and light gray marks the volitional activity. In addition, we show maximum and minimum thresholds using mean/standard deviation (red lines, $\alpha = 3$), median/MAD (green lines, $\alpha = 3$) and quantiles (blue lines, $\alpha = 95\%$), as defined in Sec. 2.1.

of the variability of a signal. The MAD for both channels is determined by

$$B_{\text{MAD},c} = m\left(\left|B_{c,1} - m_{\mathbf{B},c}\right|, \ldots, \left|B_{c,M} - m_{\mathbf{B},c}\right|\right), \tag{6}$$

where $m_{\mathbf{B},c}$ corresponds to the median of $\mathbf{B}_c$. The thresholds are then defined as

$$\begin{aligned} th_{max_c} &= m_{\mathbf{B},c} + \alpha B_{\text{MAD}_c}, \\ th_{min_c} &= m_{\mathbf{B},c} - \alpha B_{\text{MAD}_c}, \end{aligned} \tag{7}$$

where $\alpha > 0$ is again a tuning parameter. Green lines in Fig. 2 illustrate an example of maximum and minimum thresholds using median and MAD for $\alpha = 3$.

Defining thresholds by quantiles The previous methods set the thresholds symmetrically with respect to the mean and median, and do not take asymmetries in the possibly time-varying artifact into account. The next method is based on quantiles, which are the cut points dividing the probability distribution into contiguous intervals with equal probabilities. By defining the maximum and minimum thresholds as

$$th_{max_c} = \alpha\text{-quantile}(\mathbf{B}_c), \\ th_{min_c} = (100-\alpha)\text{-quantile}(\mathbf{B}_c), \quad (8)$$

we properly consider the asymmetry of the stimulation artifacts. Here, α is usually set between 90% and 98.5%. Larger values would return the maximal and minimal values of the raw EMG inside the buffer that is not desired. Blue lines in Fig. 2 illustrates an example of maximum and minimum thresholds using quantiles for $\alpha = 95\%$.

2.2 Extraction of the inter-pulse intervals (IPI)

Clustering To identify the last complete or incomplete IPI during active FES, we cluster the found potential stimulation artifacts. If two artifacts are less than $\lceil 0.1L \rceil$ samples apart then the samples between them are also marked, creating the vector $\mathbf{v}_r$ of found potential stimulation artifacts as seen in Fig. 1(b). The number of clusters should relate to the number of expected stimulation artifacts during the time period of the buffer. However, noisy signals can increase or even decrease the number of found clusters. Therefore, we use a base vector $\mathbf{v}_b$ of expected clusters to compare with the vector $\mathbf{v}_r$. The base vector is constructed with the knowledge of the stimulation frequency and the channel individual state of pulse generation (on/off).

Figure 1(c) shows the base vector construction, we expect three clusters which are L samples apart. The duration of each expected cluster is set to average durations of the clusters present in $\mathbf{v}_r$.

Cross-correlation and α-adaptation To reject wrong clusters and to reconstruct missing clusters, the cross-correlation between $\mathbf{v}_r$ and $\mathbf{v}_b$ is determined. Afterwards, the base vector is aligned to $\mathbf{v}_r$, and the corresponding IPI is extracted based on the shifted base vector.

The parameter α is adjusted at the stimulation frequency by comparing the number of found and expected clusters in the buffer. For the mean/standard deviation and median/MAD method, α is decreased by 10% if fewer clusters are found than expected, and increased by 10% if more clusters are found. For the quantiles, α will be adapted by $\pm$ 1% and will be limited to the range [90%,98.5%]. For all methods, the adaption only increases α if we find a difference greater than two between present and expected clusters.

Plausibility check The finally extracted IPIs are checked for plausibility. As the artifact should occur in the beginning of the vector, we considered the artifact detection and IPI extraction as correct when the maximum or minimum peak of the double differentiated EMG is located in the first 3 ms of the IPI.

2.3 Filtering of the found IPI

To evaluate the applicability of the EMG extraction, we also implemented a filtering block in Simulink to estimate volitional and evoked EMG activity during active FES from the returned IPI vectors. The user selects (1) the stimulation and EMG frequencies, and (2) the intervals within the IPI for assessing the volitional and evoked EMG activity. As illustrated in Fig. 2, after the artifact the M-wave usually contains information about the evoked EMG signal (medium gray area), and the M-wave tail includes information on the volitional EMG (light gray area). For these subintervals, the block estimates volitional and evoked EMG activity, respectively. We implemented different filter methods described in (Ambrosini et al., 2014; Schauer et al., 2016; Klauer et al., 2016). As volitional activity is found on the tail of the extracted IPI, it can only be evaluated from the last complete IPI.

3. EXPERIMENTAL EVALUATION

3.1 Experimental Setups

We evaluated the developed stimulation artifact detection using EMG data from FES-assisted gait training. We conducted the experiments with two healthy subjects each one using a different hardware setup (Figure 3 illustrates the general configuration) since the artifact detection should be used with different non-hardware-synchronized stimulators and EMG amplifies. Only one leg was stimulated at the tibialis anterior (TA) and gastrocnemius (GAS) muscles using hydro-gel electrodes (ValuTrode®, Axelgaard Manufacturing Co., Ltd., USA), while we measured EMG at the same muscles using AgCl electrodes (Ambu® Neuroline 720, Ambu A/S, Denmark).

The EMG electrodes are placed perpendicular to the muscle fiber direction on the stimulated leg to minimize the size of the M-wave that is induced by FES. The reference electrode is placed over a bony prominence at the knee or ankle joint of the same leg. The FES was administered in synchronization with the gait cycle using a velocity-adaptive real-time gait phase detection (GPD) (Seel et al., 2014; Müller et al., 2015) based on an inertial sensor at the foot to trigger the stimulation. Four gait phases (foot flat, pre-swing, swing phase, loading response) and four gait events (full contact, heel rise, toe-off, initial contact) are detected. The TA is activated shortly before the toe off (10% of the estimated gait cycle duration) and until heel strike to support the lifting of the foot during the swing phase. The GAS is stimulated to support push-off before the heel off (20% of the estimated gait cycle duration) until toe off. We set stimulation frequency to 25 Hz, while adjusting the pulse width pw and current amplitude I in real-time for the biphasic pulses. To enable a robust detection of stimulation pulse instants and IPIs, we also stimulate the muscles at a sub-sensory level ($I =$ 6mA, $pw = 50\mu$s), i.e., when no functional stimulation at a sensory or motor level occurs.

For acquiring data and for controlling stimulation, interface blocks have been programmed in Simulink for all devices, and real-time code generation is performed using the Linux Target for Simulink Embedded Coder®.

Setup A - RehaIngest For Setup A, we used one wireless Bluetooth inertial sensor (RehaGait, Hasomed GmbH, Germany) and one two-channel EMG recording device (RehaIngest, Hasomed GmbH, Germany) with Galvanically isolated USB interface. We measured the EMG at 4000 Hz, and the IMU accelerations and angular rates at 50 Hz. For stimulation, we used a current-controlled multi-channel stimulator (RehaMove3, Hasomed GmbH, Germany) with a galvanically isolated USB interface.

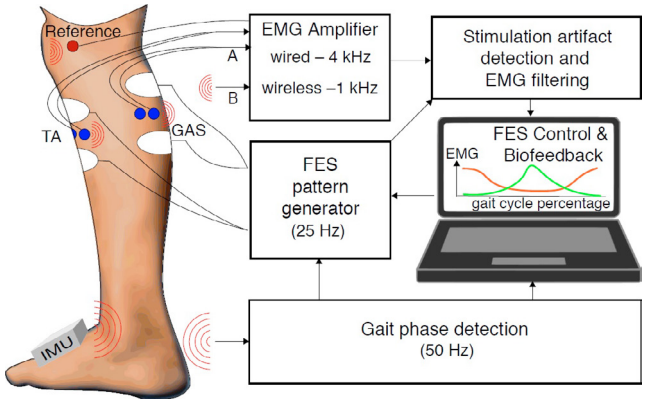

Fig. 3. Schematic representation of the setup with stimulation and EMG recording of tibialis anterior (TA) and gastrocnemius (GAS). The FES is timed by an inertial measurement unit (IMU) at the foot.

Setup B - MUSCLELAB For Setup B, we used one wireless inertial sensor and one wireless EMG sensor with an average transmission latency of 50 ms (MUSCLELAB^{TM}, Ergotest Innovation A/S, Norway). The EMG sensor features two bipolar measurement channels. We measured the EMG at 1000 Hz, and the IMU accelerations and angular rates also at 50 Hz. For stimulation, we used a current-controlled multi-channel stimulator (RehaStim I, Hasomed, Germany) with a galvanically isolated USB interface.

Experimental procedure The volunteers walked on a treadmill at slow walking speed (2 km/h) first without sensory or motor level stimulation. Then the *pw* and *I* were both linearly increased for both channels until the subject reported sensation of stimulation pulses (sensory level stimulation). In setup A, we manually increased the intensities until visible muscle contraction (motor level stimulation). For all levels of stimulation intensity the subjects walked (1) normally, (2) with emphasized push-off (more GAS activity expected), and (3) with emphasized dorsiflexion (more TA activity expected). The different gait patterns caused changes in the form and in the amplitude of the stimulation artifacts to challenge the artifact detection. Table 1 shows the applied stimulation intensities.

Table 1. Stimulation levels of tibialis anterior (TA) & gastrocnemius (GAS) for setups A and B.

	Sub-sensory (A/B)	Sensory (A)	Sensory (B)	Motor (A)
pw [μs]	50	GAS: 227 TA: 176	GAS: 226 TA: 200	GAS: 490 TA: 279
I [mA]	6	GAS: 23 TA: 19	GAS: 22 TA: 20	GAS: 49 TA: 29

3.2 Evaluation

We evaluated the artifact detection block with the recorded data from the experiments for all methods with and without α-adaptation. The percentage of IPIs that passed the plausibility check (cf. Sec. 2.2.1) directly relates to the performance of the different methods and parameters settings. Furthermore, we observed the validity of the filtering outputs (volitional and evoked) in real-time. We also counted real-time errors due to computation times that exceeded the sampling time.

4. RESULTS

We employed the artifact detection on data from both gait experiments, and then evaluated the percentage of complete IPIs that passed the plausibility check for both TA and GAS channels. Table 2 resumes the performance of the mean/standard deviation, median/MAD and quantiles for different values of α. For mean/standard deviation and Median/MAD, we set $\alpha = 3$ as suggested by (Leys et al., 2013) as a very conservative value. For the quantiles, we set α to 95%, 96%, 97% and 98% to compare performance on different α. We also evaluated the α-adaptation of the three methods. All results refer to the last complete IPIs, yet the incomplete IPIs showed very similar results.

The artifact detection and EMG filtering methods were real-time capable as we did not observe a real-time error. The filtering results showed that the visually observed volitional muscle activity of the TA and GAS with respect to the detected gait phases were as described in (Perry and Burnfield, 2010).

Table 2. Gait experiment: Artifact detection success rate for GAS and TA (complete IPI).

	RehaIngest	MUSCLELAB
Mean/std	$\alpha = 3$	$\alpha = 3$
GAS	98.93%	94.92%
TA	98.57%	94.48%
Mean/std α-adaptation	$\overline{\alpha} = 1.37$	$\overline{\alpha} = 2.01$
GAS	99.75%	96.09%
TA	99.69%	96.21%
Median/MAD	$\alpha = 3$	$\alpha = 3$
GAS	54.86%	87.32%
TA	52.55%	90.08%
Median/MAD α-adaptation	$\overline{\alpha} = 75.82$	$\overline{\alpha} = 18.11$
GAS	99.83%	97.88%
TA	99.79%	97.50%
Quantiles	$\alpha = 95\%$	$\alpha = 95\%$
GAS	74.21%	96.53%
TA	69.33%	97.36%
Quantiles	$\alpha = 96\%$	$\alpha = 96\%$
GAS	91.74%	97.50%
TA	87.03%	97.85%
Quantiles	$\alpha = 97\%$	$\alpha = 97\%$
GAS	98.22%	97.59%
TA	96.34%	97.62%
Quantiles	$\alpha = 98\%$	$\alpha = 98\%$
GAS	99.89%	84.96%
TA	99.81%	85.37%
Quantiles α-adaptation	$\overline{\alpha} = 98\%$	$\overline{\alpha} = 97\%$
GAS	99.69%	95.54%
TA	99.60%	96.46%

5. DISCUSSION AND CONCLUSIONS

Setup A with RehaIngest exhibited slightly higher success rates when compared to MUSCLELAB. This difference is most likely due to the lower EMG frequency of MUSCLELAB (1000 Hz) and wireless connection. Hence, the artifacts are sometimes not sampled at their maximal or minimal values and appear therefore smaller that negatively affects the detection.

Even with this discrepancy, the mean/standard deviation and the quantiles with $\alpha = 97\%$ accomplished success rates higher than 95% for both systems without the α-adaptation. For the median/MAD method, the low success rate at $\alpha = 3$ indicates that this default setting is inappropriate for EMG signals during FES. The green lines from Fig. 2 confirm the too small thresholds for the median/MAD method. Likewise, the α-adaptation reinforce this argument, by settling on a much higher average α ($\overline{\alpha} = 75.8249$ for RehaIngest, and $\overline{\alpha} = 18.1106$ for MUSCLELAB).

Also, the divergent results from the quantiles indicate that each system/data set has its own optimal α value ($\alpha = 98\%$ for RehaIngest, and $\alpha = 97\%$ for MUSCLELAB). All three threshold-selection methods exhibited success rates higher than 95% for both systems with α-adaptation. The quantiles presented a slightly lower result for the MUSCLELAB due to a higher sensitivity to adjustments compared to the mean/standard deviation and median/MAD. Furthermore, the α-adaptation avoids the manual calibration and also reacts to unexpected signal behavior during online execution. Therefore, independently of the method chosen, we recommend the α-adaptation.

Contrary to what literature advises (Leys et al., 2013), the mean/standard deviation, and median/MAD methods present similar success rates for suitable α. Considering the planned implementation of the artifact detection into a wireless EMG sensor with ARM Cortex M4 microcontroller, we must acknowledge that the median/MAD and quantiles methods demand vector sorting, which critically depends on the buffer size M. Therefore, the mean/standard deviation method with the cross-correlation and α-adaptation seems more suitable for the requirements of automatically detecting stimulation artifacts within EMG signals on a microcontroller.

The presented paper targeted stimulation artifact detection for non-hardware-synchronized stimulators and EMG amplifiers supporting the evoked and volitional estimation. For future experiments, we should also evaluate more cases (i.e., hardware, application, and subjects). We should also include further evaluation of the buffer size M, the parameters of the α-adaptation and the clustering parameters concerning the computational effort in the microcontroller and the performance of artifact detection. A larger M would e.g. improve the results of the cross-correlation but increase demands on memory and computational power.

REFERENCES

Ambrosini, E., Ferrante, S., Schauer, T., Klauer, C., Gaffuri, M., Ferrigno, G., and Pedrocchi, A. (2014). A myocontrolled neuroprosthesis integrated with a passive exoskeleton to support upper limb activities. *Journal of Electromyography and Kinesiology*, 24(2), 307–317. doi: 10.1016/j.jelekin.2014.01.006.

Arafat, S. and Skubic, M. (2008). Modeling fuzziness measures for best wavelet selection. *IEEE Transactions on Fuzzy Systems*, 16(5), 1259–1270. doi: 10.1109/tfuzz.2008.924326.

Klauer, C., Ferrante, S., Ambrosini, E., Shiri, U., Dähne, F., Schmehl, I., Pedrocchi, A., and Schauer, T. (2016). A patient-controlled functional electrical stimulation system for arm weight relief. *Medical Engineering & Physics*, 38(11), 1232–1243. doi: 10.1016/j.medengphy.2016.06.006.

Klauer, C., Raisch, J., and Schauer, T. (2012). Linearisation of electrically stimulated muscles by feedback control of the muscular recruitment measured by evoked EMG. In *2012 17th International Conference on Methods & Models in Automation & Robotics (MMAR)*. IEEE. doi:10.1109/mmar.2012.6347902.

Knaflitz, M. and Merletti, R. (1988). Suppression of stimulation artifacts from myoelectric-evoked potential recordings. *IEEE Transactions on Biomedical Engineering*, 35(9), 758–763. doi:10.1109/10.7278.

Leys, C., Ley, C., Klein, O., Bernard, P., and Licata, L. (2013). Detecting outliers: Do not use standard deviation around the mean, use absolute deviation around the median. *Journal of Experimental Social Psychology*, 49(4), 764–766. doi:10.1016/j.jesp.2013.03.013.

Lynch, C.L. and Popovic, M.R. (2012). A Comparison of Closed-Loop Control Algorithms for Regulating Electrically Stimulated Knee Movements in Individuals With Spinal Cord Injury. *IEEE Transactions on Neural Systems and Rehabilitation Engineering*, 20(4), 539–548.

Merlo, A., Farina, D., and Merletti, R. (2003). A fast and reliable technique for muscle activity detection from surface EMG signals. *IEEE Transactions on Biomedical Engineering*, 50(3), 316–323. doi: 10.1109/tbme.2003.808829.

Müller, P., Seel, T., and Schauer, T. (2015). Experimental evaluation of a novel inertial sensor based realtime gait phase detection algorithm. In *Proc. of the 5th European Conference on Technically Assisted Rehabilitation - TAR 2015*. Berlin, Germany.

Perry, J. and Burnfield, J. (2010). *Gait Analysis: Normal and Pathological Function*. Slack Inc.

Schauer, T., Seel, T., Bunt, N., Müller, P., and Moreno, J. (2016). Realtime EMG analysis for transcutaneous electrical stimulation assisted gait training in stroke patients. *IFAC-PapersOnLine*, 49(32), 183–187. doi: 10.1016/j.ifacol.2016.12.211.

Schauer, T. (2017). Sensing motion and muscle activity for feedback control of functional electrical stimulation: Ten years of experience in Berlin. *Annual Reviews in Control*, 44, 355–374. doi:10.1016/j.arcontrol.2017.09.014.

Seel, T., Landgraf, L., Escobar, V.C., and Schauer, T. (2014). Online gait phase detection with automatic adaption to gait velocity changes using accelerometers and gyroscopes. *Biomedical Engineering*, 59(s1), S795–S798. doi:10.1515/bmt-2014-5011.

Shalaby, R., Schauer, T., Liedecke, W., and Raisch, J. (2011). Amplifier design for EMG recording from stimulation electrodes during functional electrical stimulation leg cycling ergometry. *Biomedizinische Technik. Biomedical Engineering*, 56(1), 23–33.

Soares, S.B., Coelho, R.R., and Nadal, J. (2013). The use of cross correlation function in onset detection of electromyographic signals. In *2013 ISSNIP Biosignals and Biorobotics Conference: Biosignals and Robotics for Better and Safer Living (BRC)*. IEEE. doi: 10.1109/brc.2013.6487470.

Thorsen, R. (1999). An artefact suppressing fast-recovery myoelectric amplifier. *IEEE Transactions on Biomedical Engineering*, 46(6), 764–766. doi:10.1109/10.764955.